Article

Journal of
Nanoscience and Nanotechnology
Vol. 14, 4858–4864, 2014
www.aspbs.com/jnn

The c(RGDyK)-Conjugated Fe_3O_4 Nanoparticles with High Drug Load for Dual-Targeting Integrin $\alpha_v\beta_3$-Expressing Cancer Cells

Lin Guo[1,*], Wence Ding[1], and Li-Min Zheng[2]

[1] *Key Laboratory of Mesoscopic Chemistry of MOE and School of Chemistry and Chemical Engineering, Nanjing University, Nanjing 210093, P. R. China*
[2] *State Key Laboratory of Coordination Chemistry, Nanjing University, Nanjing 210093, P. R. China*

A novel drug delivery system c(RGDyK)-modified Fe_3O_4 nanoparticles with high DOX load (R-DMP), which combines magnetic targeting, integrin $\alpha_v\beta_3$ targeting and high drug loading properties, was developed by chemical coupling both doxorubicin and peptide c(RGDyK) on the synthetic dual function magnetic nanoparticles (DMP) using a multi-hand cross-linker poly-L-glutamic acid. R-DMP has high drug loading ratio and trapping efficiency for magnetic targeting, and the drug loading ratio can be controlled by adjusting the reactant ratio. Moreover, R-DMP presents narrow size distribution and is sensitive to pH for drug releasing. Compare with those of doxorubicin coupled DMP without peptide c(RGDyK) modification, D-DMP shows enhanced uptake by integrin $\alpha_v\beta_3$ targeting expressing tumor cells and displays stronger cancer cell cytotoxicity. This investigate provides a new approach for the dual-targeted delivery of therapeutic agents to tumors with controlled low carrier toxicity and high efficiency.

Keywords: Fe_3O_4, Nanoparticles, High Drug Load, c(RGDyK), Targeting.

1. INTRODUCTION

Targeted delivery of drugs can centralize anticancer agents at the desired sites and therefore reduce the systemic toxicity and enhance the therapeutic efficacy. The development of effective treatment strategies for targeted drug delivery is therefore of vital importance. Magnetic drug targeting is one of the highly valued approaches to local target tumors treatment.[1–3] In this strategy, the chemotherapeutic agent is immobilized in magnetic nano- or microspheres. By adding an external magnetic field, the chemotherapeutic agent can be retained at the target site of drug action and therefore raises drug levels at this site and avoids the drug accumulation in healthy tissues. Furthermore, the improved target selectivity as well as the enhanced duration of drug exposure to the target site result in the decrease of the overall amount of drug taken up by the reticuloendothelial system. The perfect magnetic drug carrier for magnetic drug targeting generally has characters of high drug loading, suitable size, low toxicity and well dispersion.Various magnetic nanoparticles modified with different layers, such as polymer,[4–6] lipids[7] and silanes[8] have been developed for target drugs delivery, and achieved great success in both *in vitro* and *in vivo* applications. Through these surface modification methods, the prepared magnetic drug conjugates can avoid agglomeration, improve stability, control microsphere size and facilitate to connect with other functional groups. However, the drug immobilization efficiency is generally low (the drug loading ratio is in most time less than 20%) because of the limitation of the content of functional groups in the surface of nanoparticles. The low drug loading capability necessitates the use of a large quantity of carrier that can lead to problems with carrier toxicity, metabolism, and biodegradation.[9]

Another effective treatment for targeted drug delivery relies on the receptor-mediated endocytotic pathway for internalizing into cells.[10, 11] Ligand immobilized nanoparticle can target the corresponding receptor over-expressed on the surface of tumor cell and promise intracellular drug delivery via receptor-mediated endocytosis, which

*Author to whom correspondence should be addressed.

1533-4880/2014/14/4858/007 doi:10.1166/jnn.2014.8691

improving cellular and nuclear drug uptake in tumors. Various targeting ligands, such as peptides, antibodies, proteins or small molecules have been coupled to the nanoparticle carriers for increasing drug deliver efficient.[12–14] By incorporating the designs of environment response mechanisms in drug carrier, such as acidic pH or enzymatic cleavage in the endosomes/lysosomes, anticancer drugs can be released intracellularly and targeted to specific organelles.[15, 16]

Integrin $\alpha_v\beta_3$ plays an important role in tumor angiogenesis and metastasis.[17] It is upregulated in invasive tumor cells, such as glioblastoma, melanoma, breast, ovarian, and prostate cancers, but not in quiescent endothelium and normal tissues.[18–19] Its expression on carcinoma cells potentiates metastasis by facilitating invasion and movement across blood vessels. The cyclized RGD peptide c(RGDyK) has been proven to target specifically to different tumor cells expressing cell adhesion molecule integrin $\alpha_v\beta_3$.[13, 20] Suitably modified with cyclized RGD peptide provides a special means for nanocarriers entering into the cells.

Here, we developed a drug delivery system with combined three advantages: magnetic targeting, integrin $\alpha_v\beta_3$ targeting and high drug loading. In this system, a carboxyl- together with protected amino group-modified dual functional Fe_3O_4 nano particle (DMP) has been synthesized as carriers. c(RGDyK) is chemical coupled to the carrier for special integrin $\alpha_v\beta_3$-targeting. Doxorubicin (DOX), which has a broad spectrum of antitumor properties in therapy, was used as anticancer agents. By using a novel multi-hand cross-linker poly-L-glutamic acid (PLGA), DOX can be efficiently coupled to the carrier, and an efficient approach for generating c(RGDyK)-modified Fe_3O_4 nanoparticles with high DOX load (R-DMP) for dual-targeting integrin $\alpha_v\beta_3$- expressing tumor cells has been developed.

2. MATERIALS AND METHODS

2.1. Materials and Instruments

Doxorubicin hydrochloride and Poly-L-glutamic acid (PLGA) were purchased from Sigma Company (USA). Peptide c(RGDyK) was provided by ChuTai biocompany (Shanghai, China). N-(3-Dimethylaminopropyl)-N'-ethylcarbodiimide hydrochloride (EDC) was purchased from Sigma Company (USA). U87MG cell was obtained from the Type Culture Collection of the Chinese Academy of Sciences (Shanghai, China). Follow reagents were used in the cell culture and MTT experiment: RMPI1640 RMPI1640 was purchased from Gibco Company (Grand Island, NY). Fetal bovine serum was purchased from Sijiqing Company (Hangzhou, China). Thiazolyl blue (MTT) and Dimethyl sulfoxide (DMSO) were obtained from Amresco Company (Boise, USA). All other chemicals were analytical grade.

UV-visible spectrum was recorded on a Shimadzu UV-3100 spectrophotometer (Kyoto, Japan). The ATR-IR spectrum was measured by an IFS-66V FT-IR spectrometer (Bruker Optics, Germany). Transmission electron micrographs of the products were captured on a JEOL Model JEM-200CX (Tokyo, Japan). Size analysis was performed by a BI-SM200 dynamic light scattering instrument (BrookHaven Instruments Corp., Long Island, USA). Magnetic measurements were acquired using a vibrating sample magnetometer from Quautum Design MPMS-XL7 SQUID Magnetometer (USA). The zeta potential was obtained by a NANO-Z zeta potential instrument (Malvern, USA.). The fluorescent images were measured by a Zeiss LSM 710 fluorescent microscope (German). Flow cytometry was carried out by a BD FACSCANT-OTM Flow Cytometer (BD company, USA).

2.2. Synthesize of N-phthaloyl-L-glutamic Acid Anhydride (GA)

0.025 mol phthalic anhydride and 0.025 mol L-glutamic acid were mixed in a tube and heated up to liquate and then for 15 min reaction. After cooling, the product was recrystallized by ethanol-aqueous solutions and dried at 40 °C in vacuum for 24 h. Then 2.13 mL acetic anhydride was added to the product obtained above and reflux for 15 min, the product GA was obtained after recrystallized and dried at 40 °C in vacuum for 24 h.

2.3. Generating of DMP

Superparamagnetic nanoparticles (Fe_3O_4) was obtained by the coprecipitation of $FeCl_2$ and $FeCl_3$ under basic conditions as reported by Stroeve et al.[21] The particle surface was then transformed to SiO_2 shell covered by a sol–gel process[22] using tetraethyl orthosilicate (TEOS). 100 mg obtained product was suspended in absolute ethanol curtaining ammonia solution. Then 200 mg GA and 3-aminopropyltrimethoxysilane (APS) were added respectively. After the magnetite suspension was sonicated 5 min, the mixture was stirred for at 40 °C for 12 h. After washed with absolute ethanol three times and dried at 40 °C in vacuum, the DMP product was obtained.

2.4. Preparation of R-DMP

10 mg DMP was suspended in 10 ml PBS solution and incubated with 5 mg 1-ethyl-3-[3-dimethylaminopropyl] carbodiimide hydrochloride (EDC) and 5 mg N-hydroxysuccinimide (NHS). After washing one time by PBS, 5 mg PLGA was added for reaction with DMP through impulse sonication for 2 h (each time ultrasonic bathing lasted 1 min with an interval of 5 min) at room temperature. The PLGA modified DMP was collected by a Nd–Fe–B magnet, and the supernatant solutions were removed. Then 10 mL 0.1 M PBS solution was added to get rid of the residual PLGA. After washing three times the particle was incubated with 5 mg EDC, 5mg NHS and DOX solution (1 mg/mL) in 10 mL PBS solution by impulse sonication for 3 h at room temperature. The product was

washed carefully until the supernatant solutions displayed no reddish color. Then 20 μl hydrazine hydrate solution was added in and the mixture was incubated by impulse sonication for 10 min at room temperature. After washed with PBS, 200 μl c(RGDyK) peptide (4 mg/ml) solutions, which pre-treated with 5 mg EDC and NHS, were added and reacted by impulse sonication for 2 h. Then the products were collected using a magnet and washed several times. R-DMP products were finally obtained by freeze-drying.

2.5. Evaluation of the Amount of DOX and Peptide

R-DMP was distributed in 10 mL PBS solutions, 0.2 mL R-DMP suspensions were taken out and dissolved in 0.5 ml 36–38% hydrochloric acid followed by the addition of 1.3 ml 75% ethanol. The dissolved R-DMP solution was diluted with 10 mL distilled water, and its UV-visible spectrum was then recorded. The amount (A) of DOX coupled to DMP was calculated using a standard curve for DOX in 1:2 hydrochloric acid and ethanol solution: $y = 44.96x$, where y is the concentration of DOX (μg/ml), and x is the absorption of DOX at 479 nm. The DOX loading ratio (R) was calculated according to the following equation:

$$R(\%) = A/(A + 1000) \times 100$$

where A is the amount of the DOX coupled to DMP.

The amount of c(RGDyK) peptide attached to DMP was obtained by measuring the UV-visible absorption of c(RGDyK) peptide at 260 nm using a standard curve for peptide PBS solution mixed with EDC and NHS: $y = 21.68x$, where y is the concentration of peptide (μg/ml), and x is the absorption of peptide at 260 nm.

2.6. Observation of Cellular Uptake of the R-DMP

U87MG cell suspensions (1×10^4 cells) were seeded in a bottom hole culture dish (0.13 mm glass) for 12 h. The cells were then incubated with 2 μg of reagents for 2 h. After the incubation, the U87MG cells were washed three times with PBS solution before being examined by a fluorescent microscope.

2.7. *In Vitro* DOX Release Studies

The test of DOX release from R-DMP was performed in test tubes with stirring speed of 60 rpm. The DOX content in the supernate of each tube was measured every 8 h after incubating by UV-Visible spectra.

2.8. MTT Cytotoxicity Assays

The MTT assay was used to measure cytotoxicity of different drug concentrations as previously described.[23] All assays were performed at least three times in quintuplicate. The cytotoxicity was calculated using the following formula:

$$\text{Cytotoxicity} = [1 - (\text{absorbance of experimental wells})/ \times (\text{absorbance of control wells})] \times 100$$

3. RESULTS AND DISCUSSION

3.1. Generation of R-DMP

The process for generating R-DMP is shown in Figure 1. Both carboxyl and protected amino groups modified dual functional magnetic nano particle (DMP) has been synthesized by coupling GA with DMP at first. Amino acid polymer PLGA, which has large numbers of carboxyl groups together with an end-amino group, is then coupled to the surface of DMP. Consequently, large amount of carboxyl groups is introduced on the surface of DMP. Through the PLGA single-to-multi amino groups method, DOX can be efficiently immobilized on the nanoparticles through amide bond. Finally, c(RGDyK) is coupled with DMP through amide bond after deprotection of amino groups of DMP.

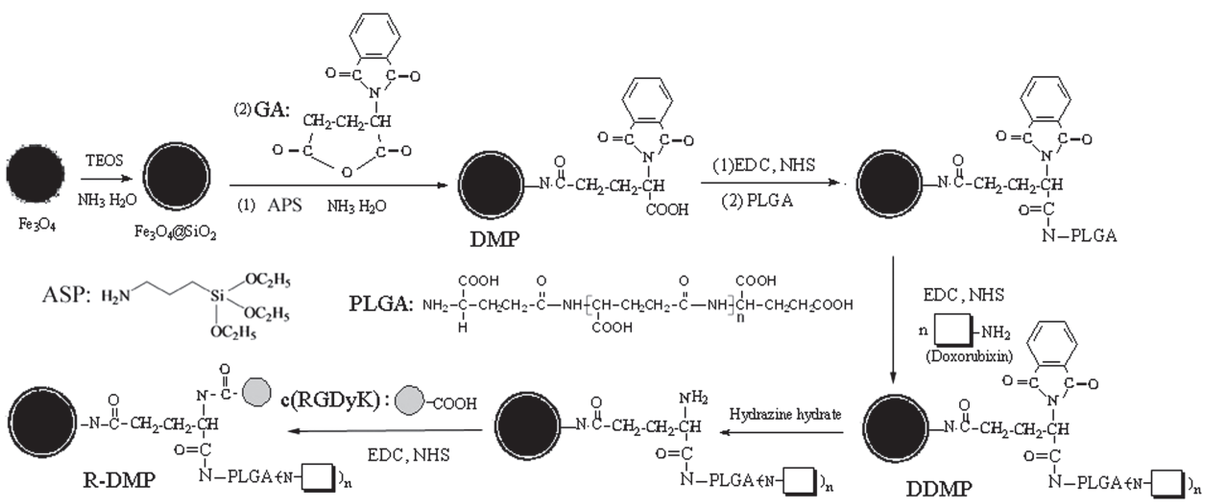

Figure 1. Procedure for R-DMP generation.

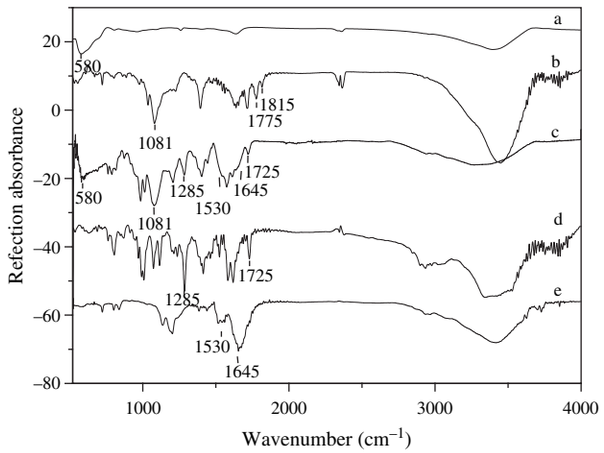

Figure 2. ATR-IR spectra of different products. (a) Fe_3O_4; (b) DMP; (c) R-DMP; (d) DOX; (e) c(RGDyK).

The structure properties of R-DMP products are characterized by attenuated total reflection infrared (ATR-IR) spectroscopy. Figure 2(c) shows that R-DMP has a typical Fe–O stretching vibration band around 580 cm^{-1}, indicating the product contain magnetite. Formation of the silane layer on the surface of nanoparticles was confirmed by the band at 1118 cm^{-1} corresponding to the Si—O—Si bond. The strong bond observed at 1725 cm^{-1} and 1285 cm^{-1} are owing to the 13-carbonyl(—C═O)stretching vibration and framework vibration of the —C═O on the anthracene cycle of DOX respectively, which confirms that R-DMP contain DOX. The shoulder peaks at 1645 and 1530 cm^{-1} are correspond to the characteristic amide I and amide II of the c(RGDyK)-peptide. Two peaks at 1750-1880 cm^{-1} of DMP assigned to the carboxyl group of acid anhydride (Fig. 2(b)) disappeared after reaction with DOX and c(RGDyK)-peptide (Fig. 2(c)). These results indicate that (RGDyK)-peptide are covalently bonded on DMP. The amount of peptide coupled on the R-DMP surface was measured to be approximately 177 μg/mg DMP.

3.2. DOX Load Ratio

Plot of DOX load ratio via different DOX/DMP ratio is shown in Figure 3. It is observed that the DOX/DMP ratio (w/w) influence the drug loading ratio intensively. In the case of DOX/DMP ratio of 0.5, the drug loading ratio is only about 27.8%. With the DOX /DMP ratio increasing, the drug loading ratio increases accordingly. The highest coupling efficiency is obtained when the DOX/DMP ratio is 8. The calculated drug loading ratio is about 85.3% and approximately 5646 μg DOX could be loaded on 1 mg of DMP. This value is about 40 times greater than that of polymer lipid and micelle carriers (about 140 μg/mg).[24–26] It is also 6 times the amount loaded by using general dual cross-linker such as glutaraldehyde.[27] This behavior is due to the much more functional positions provide by PLGA for DOX to load onto DMP. With the DOX/DMP ratio further increasing, the drug loading ratio seems saturated and decreases. As higher drug loading capability can depress the problem of carrier toxicity.[9] R-DMP with low carrier toxicity, can be controlled generating by adjusting the reactant ratio.

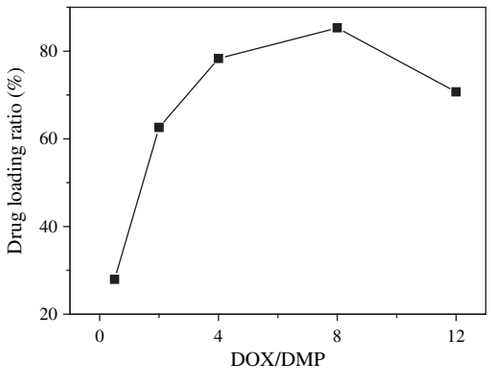

Figure 3. Plots of drug load ratio via different ratios of DOX to DMP.

3.3. Magnetic and Size Analysis

The curve of magnetization (M) versus field (H) of R-DMP (Fig. 4(a)) shows that R-DMP exhibits superparamagnetic property at room temperature, which is an improtant property for magnetic carrier.[1, 28] When a magnet is applied to the outside of the test tube (Fig. 4(b)), R-DMP is gradually enriched at the location of the magnet, while the bulk aqueous solution eventually becomes almost colorless. These results indicate that R-DMP is capable of responding to an external magnetic field and shows high trapping efficiency for magnetic targeting. R-DMP disperses well in aqueous solution. The zeta potential of R-DMP at 25 °C is −38 mV. The well disperse of R-DMP in aqueous solutions may due to the electrostatic repulsion of the particle and the screening effect of the covered silica and PLGA layer.

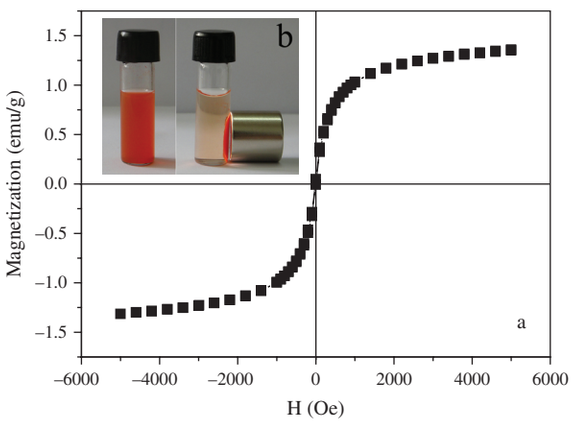

Figure 4. (a) Magnetization (M) versus field (H) curve at approximately 27 °C for R-DMP, (b) Images of R-DMP-suspended aqueous solution 1 h after a magnet is placed outside the test tube.

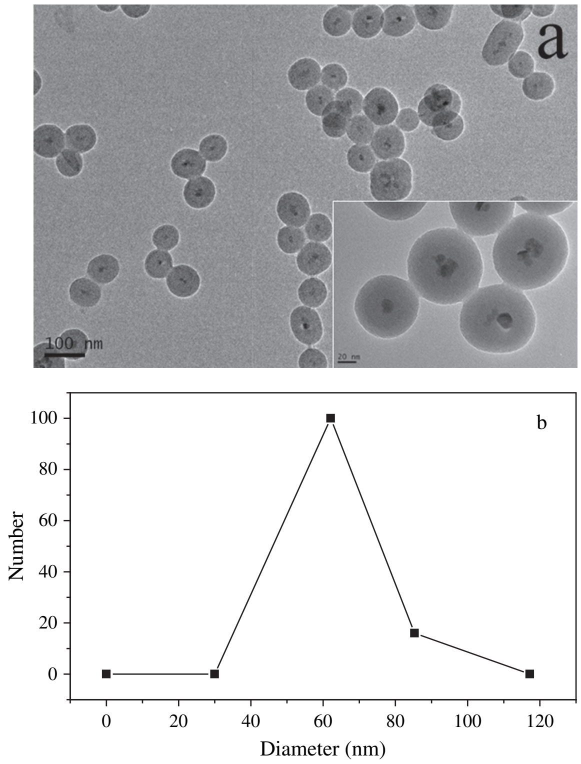

Figure 5. (a) Transmission electron micrograph of R-DMP, (b) Size distribution plot obtained by dynamic light scattering of R-DMP.

The transmission electron micrograph (Fig. 5(a)) shows that the R-DMP has a typical core-shell structure. The magnetic core is composed with several Fe_3O_4 nanoparticles with diameter about 10 nm. This may be the reason for the superparamagnetic property of R-DMP. The properties of superparamagnetic magnetite can be seen from Li et al. (2009, 7: 25–34) in Geobiology.[29] The diameter of R-DMP is in the range of 50–70 nm. The size distribution of R-DMP particles obtained by using dynamic light scattering (Fig. 5(b)), reveals that R-DMP has a narrow size distribution (Fig. 5(b)). The mean diameter of R-DMP is about 70 nm. These particles were in the range of optimal size for drug carrier to evade the RES of the body as well as to penetrate small tissue capillaries and had a longest blood circulation times.[8]

3.4. Drug Release

The amount of DOX released from R-DMP nanoparticles is investigated at different pH (Fig. 6). It is observed that in all cases the burst release from the nanoparticles at an early period. The DOX release is quicker in a mildly acidic condition than in normal physiological condition. At pH 7.2, about 48.5% of original DOX releases from R-DMP after incubated for 72 h. With the pH decreases to 3.5, the released DOX increases up to 70.8%. This may due to the weak binding between DOX and the carboxylic groups of the polymer and the reprotonation of the amino groups.[30] These properties were suitable for systemic application and

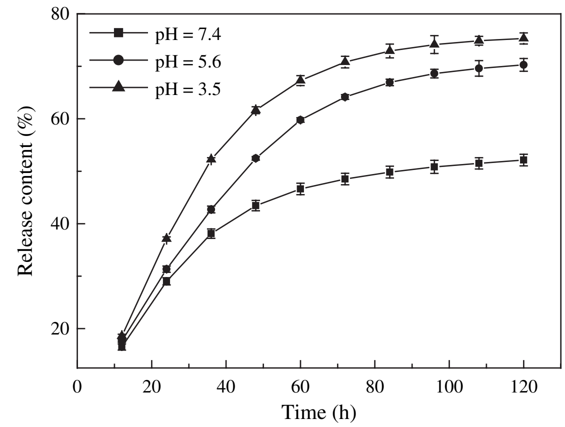

Figure 6. Doxorubicin release content of R-DMP in PBS solution with different pH at 37 °C.

were released more in acidic pH than in normal physiological condition. Therefore, this pH-dependent release function is especially useful for achieving the tumor-targeted drug delivery with nanoparticles.

3.5. Targeting Cell Uptake

The targeting uptake effect of R-DMP was evaluated by flow cytometry and confocal laser scanning microscopy (CLSM). Integrin $\alpha_v\beta_3$ expressing U87MG cancer cell was used to incubate with nanoparticle. Figure 7(a) shows the mean fluorescence intensity and the parent ratio of U87MG cell after 2 h incubating with R-DMP and only DOX coupled DMP without c(RGDyK) modification (DDMP). It is observed that R-DMP shows higher mean fluorescence intensity than that of DDMP. About 3 fold uptake increase in U87MG cell was observed with R-DMP over DDMP. The intracellular distribution and uptake of R-DMP and DDMP were also measured by CLSM. It can be seen from Figure 7(b) that the majority of the nano-particles were localized in the cytoplasmic compartments (e.g., endosomes) when they are taken into the cancer cells. The intracellular DOX fluorescence intensity of R-DMP is obviously higher than that of DDMP, indicating an increase uptake of R-DMP by the cancer cell. The enhanced cell uptake with R-DMP over DDMP was in agreement with flow cytometry results. This may due to that rapid integrin $\alpha_v\beta_3$ mediated endocytosis facilitated the internalization of R-DMP inside the cancer cells.

3.6. Antitumor Effects

The antitumor effects of R-DMP were evaluated by integrin $\alpha_v\beta_3$ expressing U87MG cell (Fig. 8). Both R-DMP and DOX coupled DMP without c(RGDyK) modification (DDMP) sample were controlled to an equal drug concentration by UV spectra before adding into the U87MG cell culture medium. Cells were then incubated for 72 h with different nanoparticle samples. The cell inhibition ratio was obtained by measuring the ratio of the amount

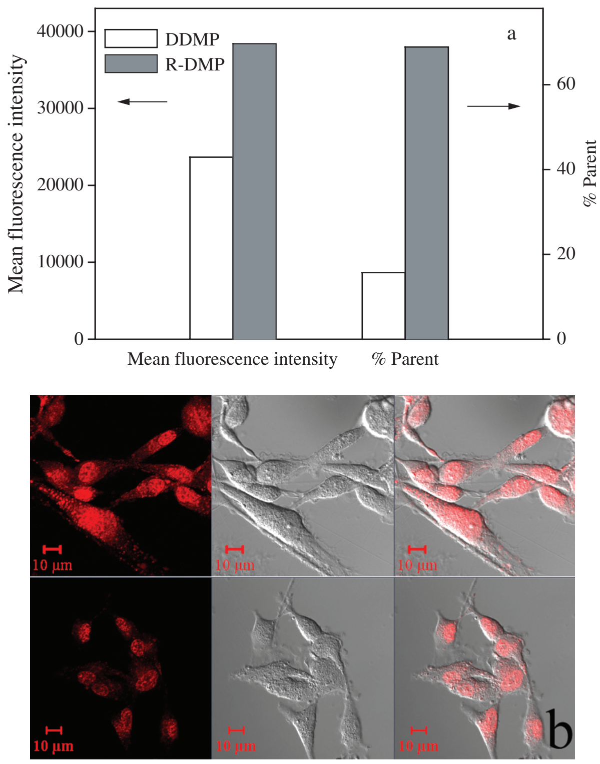

Figure 7. (a) Mean fluorescence intensity and parent % of U87MG cells after being incubated with DDMP and R-DMP for 1 h with a DOX concentration of 2 μg by flow cytometry. b: Confocal laser scanning microscopy of U87MG cells treated with R-DMP (up) and DDMP (down) in the presence of a total DOX concentration of 4 μg/mL after incubation for 2 h at 37 °C. Bars: 10 μm.

of the cells of the treated group over the untreated control. Figure 8 shows that free DMP and pure c(RGDyK) produces little inhibition of target cell growth, indicates the minimal cell cytotoxicity owing to the c(RGDyK) and DMP carrier. The inhibition ratio of R-DMP on U87MG cells is higher than that of DOX coupled DMP without c(RGDyK) modification (DDMP) on a mole-per-mole

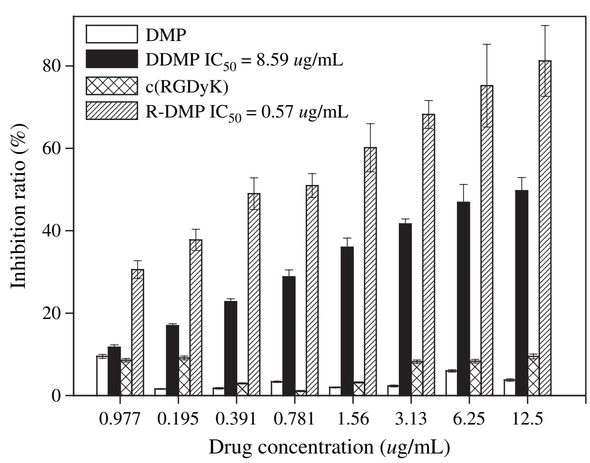

Figure 8. Cytotoxic effects of DMP, DDMP, c(RGDyK) and R-DMP in U87MG carcinoma cells.

basis. The IC_{50} value of R-DMP is also lower than that of DDMP correspondingly. These behaviors demonstrate that the special c(RGDyK)-integrin $\alpha_v\beta_3$ targeting facilitated the uptake of R-DMP to integrin $\alpha_v\beta_3$-expressing cancer cells, which lead to raise the drug deliver effect.

4. CONCLUSION

In conclusion, c(RGDyK)-modified Fe_3O_4 nanoparticles with high DOX load was generated for dual-targeting integrin $\alpha_v\beta_3$-expressing carcinoma cells. Besides the passive magnetic drug target function, the presence of c(RGDyK) on the surface provide the active receptor-target function for R-DMP. R-DMP exhibits enhanced uptake by integrin $\alpha_v\beta_3$-expressing carcinoma cells and displays stronger cancer cell cytotoxicity. Moreover, R-DMP has high drug load ratio and pH sensitive drug releasing. The drug loading ratio can be controlled by adjusting the reactant ratio. This investigate provides a new approach for the dual-targeted delivery of therapeutic agents to tumors with controlled low carrier toxicity and high efficiency.

Acknowledgment: This work was financially supported by the Natural Science Foundation of China (NSFC21073091) and Natural Science Foundation of Jiangsu Province (No. BK2009009).

References and Notes

1. M. Arruebo, R. Fernández-Pacheco, M. R. Ibarra, and J. Santamaría, *Nano Today* 2, 22 (**2007**).
2. C. Alexiou, W. Arnold, R. J. Klein, F. G. Parak, P. Hulin, C. Bergemann, W. Erhardt, S. Wagenpfeil, and A. S. Lubbe, *Cancer Res.* 60, 6641 (**2000**).
3. M. Babincova, V. Altanerova, C. Altaner, P. Cicmanec, and P. Babinec, *Med. Phys.* 31, 2219 (**2004**).
4. G. Mikhaylov, U. Mikac, A. A. Magaeva, V. I. Itin, E. P. Naiden, I. Psakhye1, L. Babes, T. Reinhecke, C. Peter, R. Zeiser, M. Bogyo, V. Turk, S. G. Psakhye, B. Turk, and O. Vasiljeva1, *Nat. Nanotechnol.* 6, 594 (**2011**).
5. Y. Y. Wan, H. L. Zhao, R. H Yu, and M. B Lan, *J. Nanosci. Nanotechol.* 12, 2456 (**2012**).
6. B. Gaihre, M. S. Khilb, D. R. Lee, and H. Y. Kimb, *Int. J. Pharm.* 365, 180 (**2009**).
7. S. Brulé, M. Levy, C. Wilhelm, D. Letourneur, F. Gazeau, C. Ménager, and C. L. Visage, *Adv. Mater.* 23, 787 (**2011**).
8. Q. Liu, J. X. Zhang, W. L. Xia, and H. C. Gu, *J. Nanosci. Nanotechol.* 12, 7709 (**2012**).
9. T. M. Allen and P. R. Cullis, *Science* 303, 1818 (**2004**).
10. D. Peer, J. M. Karp, S. Hong, O. C. Farokhzad, R. Margalit, and R. Langer, *Nat. Nanotechnol.* 2, 751 (**2007**).
11. T. R. Pearce, K. Shroff, and E. Kokkoli, *Adv. Mater.* 24, 3803 (**2012**).
12. J. M. Shen, X. M. Guan, X. Y. Liu, J. F.Lan, T. Cheng, and H. X. Zhang, *Bioconjugate Chem.* 23, 1010 (**2012**).
13. J. Xie, K. Chen, H. Y. Lee, C. Xu, A. R. Hsu, S. Peng, X. Chen, and S. H. Sun, *J. Am. Chem. Soc.* 130, 7542 (**2008**).
14. F. J. J. Toublan, S. Boppart, and K. S. Suslick, *J. Am. Chem. Soc.* 128, 3472 (**2006**).
15. T. M. Allen, *Nat. Rev. Cancer* 2, 750 (**2002**).
16. K. T. Oh, H. Yin, E. S. Lee, and Y. H. Bae, *J. Mater. Chem.* 17, 3987 (**2007**).

17. J. P. Xiong, T. Stehle, R. Zhang, A. Joachimiak, M. Frech, S. L. Goodman, M. A. Arnaout, B. Diefenbach, R. Dunker, and D. L. Scott, *Science* 296, 151 **(2002)**.
18. J. D. Hood and D. A. Cheresh, *Nat. Rev. Cancer* 2, 91 **(2002)**.
19. H. Jin and J. Varner, *Br. J. Cancer* 90, 561 **(2004)**.
20. K. Temming, D. L. Meyer, R. Zabinski, E. C. F. Dijkers, K. Poelstra, G. Molema, and R. J. Kok, *Bioconjugate Chem.* 17, 1385 **(2006)**.
21. Y. S. Kang, S. Risbud, and J. F. P. Rabolt, *Chem. Mater.* 8, 2209 **(1996)**.
22. X. Liu, Z. Ma, J. Xing, and H. Liu, *J. Magn. Magn. Mater.* 270, 1 **(2004)**.
23. C. Bliss, *Ann. Appl. Biol.* 22, 134 **(1935)**.
24. W. J. Du, Z. Q. Xu, A. M. Nystrom, K. Zhang, J. R. Leonard, and K. L. Wooley, *Bioconjugate Chem.* 19, 2492 **(2008)**.
25. S. Guo, D. Li, L. Zhang, J. Li, and E. Wang, *Biomaterials* 30, 1881 **(2009)**.
26. Y. Hu, J. Xie, Y. W. Tong, and C. H. Wang, *J. Controlled Release* 118, 7 **(2007)**.
27. L. Guo, J. Huang, X. Zhang, Y. Li, and L. M. Zheng, *J. Mater. Chem.* 18, 5993 **(2008)**.
28. M. Mary, Scientific and Clinical Applications of Magnetic Carriers, edited by U. Hafeli, W. Schutt, and M. Zborowski, Plenum, New York **(1997)**, p. 303.
29. Y. L. Li, S. M. Pfiffner, M. D. Dyar, H. Vali, K. Konhauser, D. R. Cole, A. J. Rondinone, and T. J. Phelps, *Geobiology* 7, 25 **(2009)**.
30. S. K. Sahua, S. Maitib, A. Pramanika, S. K Ghoshb, and P. Pramanik, *Carbohydr. Polym.* 87, 2593 **(2012)**.

Received: 22 February 2013. Accepted: 10 May 2013.